

Immature Hominin Craniodental Remains From a New Locality in the Rising Star Cave System, South Africa

JULIET K. BROPHY*

Department of Geography and Anthropology, Louisiana State University, Baton Rouge, LA 70803, USA; and, The Centre for the Exploration of the Deep Human Journey, University of the Witwatersrand, Private Bag 3, Wits 2050, SOUTH AFRICA; jbrophy@lsu.edu

MARINA C. ELLIOTT

Department of Archaeology, Simon Fraser University, 8888 University Drive, Burnaby, British Columbia, V5A 1S6, CANADA; and, The Centre for the Exploration of the Deep Human Journey, University of the Witwatersrand, Private Bag 3, Wits 2050, SOUTH AFRICA; mce4@sfu.ca

DARRYL J. DE RUITER

Department of Anthropology, Texas A&M University, College Station, TX 77843; Department of Anthropology, California State University-Stanislaus, Turlock 95382, CA, USA; and, The Centre for the Exploration of the Deep Human Journey, University of the Witwatersrand, Private Bag 3, Wits 2050, SOUTH AFRICA; deruiter@tamu.edu

DEBRA R. BOLTER

Department of Anthropology, Modesto Junior College, Modesto, CA 95350, USA; and, The Centre for the Exploration of the Deep Human Journey, University of the Witwatersrand, Private Bag 3, Wits 2050, SOUTH AFRICA; bolterd@mjc.edu

STEVEN E. CHURCHILL

Department of Evolutionary Anthropology, Box 90383, Duke University, Durham, NC 27708, USA; and, The Centre for the Exploration of the Deep Human Journey, University of the Witwatersrand, Private Bag 3, Wits 2050, SOUTH AFRICA; churchy@duke.edu

CHRISTOPHER S. WALKER

Department of Molecular Biomedical Sciences, College of Veterinary Medicine, North Carolina State University, Raleigh, NC 27695; Department of Evolutionary Anthropology, Box 90383, Duke University, Durham, NC 27708, USA; and, The Centre for the Exploration of the Deep Human Journey, University of the Witwatersrand, Private Bag 3, Wits 2050, SOUTH AFRICA; christopher_walker@ncsu.edu

JOHN HAWKS

Department of Anthropology, University of Wisconsin-Madison, Madison, WI 53706, USA; and, The Centre for the Exploration of the Deep Human Journey, University of the Witwatersrand, Private Bag 3, Wits 2050, SOUTH AFRICA; jhawks@wisc.edu

LEE R. BERGER

The Centre for the Exploration of the Deep Human Journey, University of the Witwatersrand, Private Bag 3, Wits 2050, SOUTH AFRICA; Lee.Berger@wits.ac.za

*Corresponding author: Juliet K. Brophy; jbrophy@lsu.edu

submitted: 17 January 2021; accepted: 6 July 2021

ABSTRACT

Homo naledi is known from the Rising Star cave system, South Africa, where its remains have previously been reported from two localities: the Dinaledi Chamber (U.W. 101) and Lesedi Chamber (U.W. 102). Continued exploration of the cave system has expanded our knowledge of the Dinaledi Chamber and its surrounding passageways (the Dinaledi Subsystem), leading to the discovery of new fossil localities. This paper discusses the fossil assemblage from the locality designated U.W. 110. This locality is within a narrow fissure of the Dinaledi Subsystem approximately 12 meters southwest of the 2013–2014 excavation. Fossil remains recovered from this locality include six hominin teeth and 28 cranial fragments, all consistent with a single immature hominin individual. The dental morphology of the new specimens supports attribution to *H. naledi*. This is the first immature individual of *H. naledi* to preserve morphological details of the calvaria in association with dental evidence. This partial skull provides information about the maturation of *H. naledi* and will be important in reconstructing the developmental sequence of immature remains from other *H. naledi* occurrences. This is the third locality described with *H. naledi* material in the Rising Star cave system and represents a depositional situation that resembles the Lesedi Chamber in some respects.

Dinaledi Subsystem

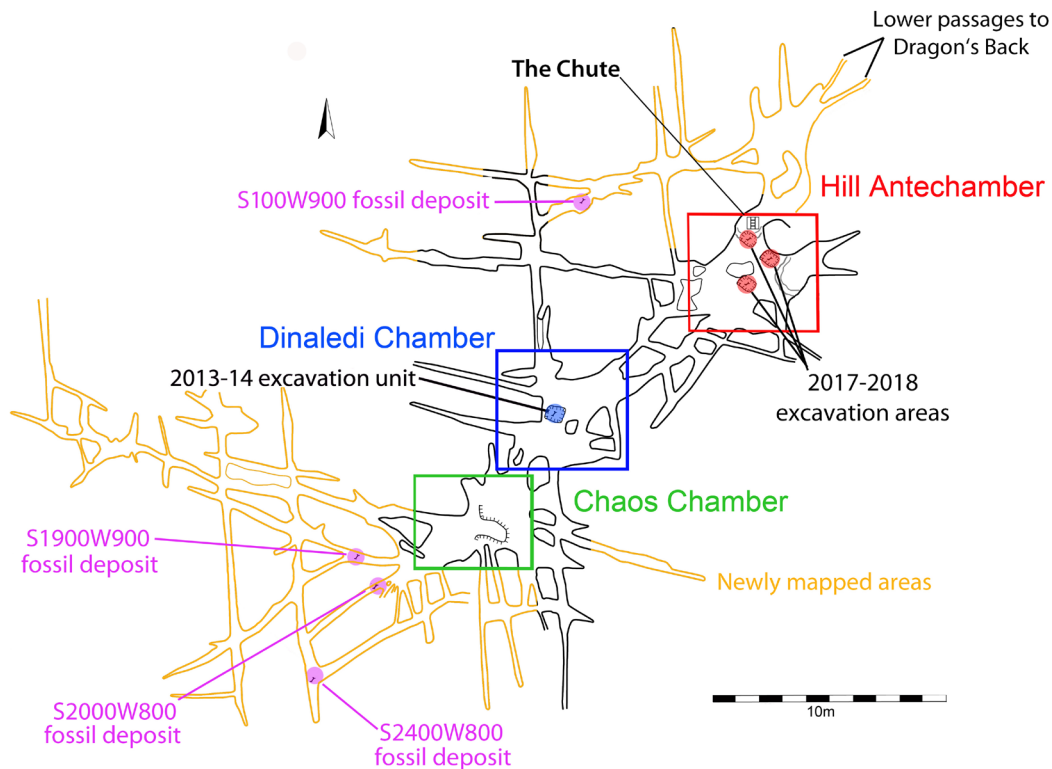


Figure 1. Map of the Dinaledi Subsystem.

INTRODUCTION

The Rising Star cave system is located in the Cradle of Humankind UNESCO World Heritage Site, Gauteng Province, South Africa. The cave system has been the site of discoveries of *Homo naledi* fossil material in the Dinaledi Chamber (U.W. 101; Berger et al. 2015) and subsequently in the Lesedi Chamber (U.W. 102; Hawks et al. 2017). Continued speleological explorations and mapping have outlined the spatial complexity of the area near and around the Dinaledi Chamber, leading to the characterization of this area of the cave system as the Dinaledi Subsystem (Elliott et al. 2021). These explorations identified new fossil localities within this subsystem, at varied distances from the Dinaledi Chamber excavations. The new fossil-bearing localities have been incorporated into a grid system imposed on the subsystem as part of ongoing excavations (Figure 1; Elliott et al. 2021).

Here, we describe the fossil material from one of these new fossil-bearing localities, located in the excavation grid system at S2000W800 (Elliott et al. 2021), that has been designated as U.W. 110 under the University of the Witwatersrand's locality numbering system (Zipfel and Berger 2009). This locality is situated within a narrow fissure, 12 meters southwest of the original 2013–2014 Dinaledi Chamber excavation, at roughly the same elevation. The team carried out only surface collection at this locality at the time of discovery in September 2017 due to the con-

straints of the immediate environment. Six hominin teeth and 28 cranial fragments were recovered. This material was scattered across the present surface of the fissure, which is approximately 15cm wide by 80cm long, and which slopes down gently in a northeasterly direction. The U.W. 110 locality can be reached only via a long and extremely narrow passage which is challenging even for the experienced caving team. Additional contextual information for this locality is presented by Elliott et al. (2021).

Multiple immature fossil remains from one species are rare in the fossil record and thus immature individuals are of particular importance. This study undertook a comparative analysis of the U.W. 110 fossil material to determine taxonomic identity, representation of individuals, morphological information, and maturational stage. The work included an anatomical description of each element and the refitting of cranial fragments. Although all of the hominin remains described in our previous work from the Rising Star cave system represent *H. naledi* (Berger et al. 2015; de Ruiter et al. 2019; Hawks et al. 2017; Laird et al. 2017; Schroeder et al. 2017), such single species representation is unusual within the hominin-bearing cave assemblages from the Cradle of Humankind (Dirks et al. 2015; Hawks et al. 2017; Martin et al. 2020; Randolph-Quinney 2015). Therefore, the new material was compared to all hominin taxa previously recovered from sites in the area. The analysis of this specimen adds to the growing dataset on ontogeny

TABLE 1. HOMININ FOSSIL MATERIAL RECOVERED FROM SITE 110.

Specimen number	Description
U.W. 110-1	maxillary right deciduous second molar (dM2)
U.W. 110-2	maxillary right fourth premolar (P4) crown germ
U.W. 110-3	cranial fragment
U.W. 110-4	cranial fragment
U.W. 110-5	maxillary right first molar (M1) crown
U.W. 110-6	cranial fragments (5)
U.W. 110-7	cranial fragment
U.W. 110-8	cranial fragment
U.W. 110-9	cranial fragment
U.W. 110-10	cranial fragment
U.W. 110-11	cranial fragment
U.W. 110-12	cranial fragment
U.W. 110-13	cranial fragments (10)
U.W. 110-14	maxillary right first incisor (I1) germ
U.W. 110-15	maxillary left second incisor (I2) germ
U.W. 110-16	cranial fragments (5)
U.W. 110-17	maxillary left deciduous second molar (dM2)

and life history of *Homo naledi* (Bolter and Cameron 2020; Bolter et al. 2020).

MATERIALS AND METHODS

Six hominin teeth and 28 cranial fragments were recovered from U.W. 110. Anatomical descriptions of the recovered craniodental material are provided below. All specimens have been given unique accession numbers beginning with U.W. 110 (Table 1). In some cases, several small fragments were found in close spatial association or physical contact and such fragments were collected together and given the same accession number. This combination of elements under one accession number relates to their close contact and not necessarily anatomical identity of each fragment; most fragments with the same accession number do not conjoin.

Each specimen was examined using a hand lens (10x magnification) and stereomicroscope. Three-dimensional meshes were generated for the surfaces of each specimen using photogrammetry. To achieve this, each specimen was placed on a turntable and photographed using a Canon 6D camera and a 75mm macro lens from 64 angles, in each of three axes of rotation. Metashape (Agisoft LLC) software

was used to compute the 3D mesh for each specimen. All specimens were compared to previously recovered *H. naledi* remains from the Dinaledi and Lesedi Chambers (Berger et al. 2015; Hawks et al. 2017), and to comparative materials housed at the Phillip V. Tobias Fossil Primate and Hominid Laboratory at the University of the Witwatersrand, as well as published data. Descriptions of the dental material follow the terminology used by Bailey et al. (2019) and Hawks et al. (2017).

RESULTS

DENTAL MATERIAL

Table 2 lists the six hominin teeth that were recovered from U.W. 110. No element is duplicated, and all are developmentally and wear-stage compatible.

U.W. 110-1: Rdm²

This specimen is a maxillary second deciduous right molar, consisting of a crown and partial roots (Figure 2). Four principal cusps are present. The tooth has moderate wear that has blunted the cusps. Wear facets and pits of dentine

TABLE 2. MESIODISTAL AND BUCCOLINGUAL (labiolingual) MEASUREMENTS FROM SITE 110.

Specimen No.	Element	MD (mm)	B(La)L (mm)
U.W. 110-1	Rdm ² crown and roots	8.86	9.5
U.W. 110-2	RP ⁴ crown	8.33	10.8
U.W. 110-5	RM ¹ crown	11.39	11.56
U.W. 110-14	RI ¹ crown	8.17	6.63
U.W. 110-15	RI ² crown	6.37	6.35
U.W. 110-17	Ldm ² crown and roots	8.77	9.45

exist on all four cusps with the largest pit on the protocone. The tooth has an ovoid mesial interproximal facet but no distal interproximal facet. The crown has a rhomboidal shape with a mesiobuccal projection of the paracone and distolingual extension of the hypocone. The paracone is positioned slightly mesial to the protocone. The cusps are arranged as protocone>paracone>metacone>hypocone. The cusp apices are widely spaced and positioned at the edge of the occlusal margin. The trigon consists of a basin with faint accessory crests emanating from the mesial aspect of the paracone and the protocone. These crests outline the distal

margin of the anterior fovea which is a BL-oriented groove. The mesial marginal ridge is thicker and higher than the distal marginal ridge, and the posterior fovea is little more than a small pit at the terminus of the fissure separating the hypocone from the metacone. The tooth exhibits a strong epicrista. Buccally, there is mild cervical prominence and a peak in the enamel between the roots. The shallow buccal groove gets deeper towards the occlusal margin. The cervical groove is weakly evident on the lingual face. The lingual groove is a narrow and deep cleft at the occlusal surface that becomes broader and shallower towards the



Figure 2. A) Locality U.W. 110-1 right maxillary deciduous second molar in buccal, lingual, distal, and mesial views. B) U.W. 110-1 (left) in occlusal view compared to a Rdm2 from the Dinaledi Chamber, U.W. 101-1687 (right).

TABLE 3. MESIODISTAL AND BUCCOLINGUAL (labiolingual) MEASUREMENTS OF MAXILLARY dm2 SPECIMENS FROM SITES U.W. 101 and U.W. 110.

Specimen No.	MD (mm)	B(La)L (mm)
U.W. 110-1	8.86	9.5
U.W. 110-17	8.77	9.45
U.W. 101-384	9.3	10.3
U.W. 101-544a	9.7	9.5
U.W. 101-1376	10.3	10.1
U.W. 101-1687	10.4	10.1

cervix. A pit and V-shaped Carabelli's feature is present on the mesiolingual corner. Enamel chipping exists on the distolingual margin of the hypocone and the mesial aspect of the mesial marginal ridge. Both of the chipped areas have smooth edges indicating chipping occurred during life.

The deciduous molar retains evidence of three widely splayed roots. The plate-like lingual root is irregularly broken at approximately three-quarters of its original length (7.8mm from cervix). The distobuccal root is broken at the cervix, while the mesiobuccal root is broken just above the cervix. All of the root remnants are stained from contact with the cave matrix. The tooth dimensions are 8.8mm MD and 9.5mm BL. The morphology and wear stage of the tooth are consistent with that of a proposed antimere, U.W. 110-17 (Ldm²). U.W. 110-1 is slightly smaller than the comparable maxillary second deciduous molars from locality 101 (Table 3).

U.W. 110-2: RP¹ crown

This maxillary right fourth premolar is represented by a crown with no root formation, indicative of a tooth in the process of development (Figure 3). The crown is partially infilled with sediment and unworn with no wear facets or dentine exposures. The occlusal outline is ovoid. The paracone is slightly larger in area than the protocone. Even unworn, the protocone is more rounded than the paracone. The protocone apex is more mesially positioned than the paracone apex. The cusps are both tall relative to the occlusal margin and approximately the same height. Mesial and distal accessory crests extend from the paracone apex and end at the longitudinal fissure. The thick mesial marginal ridge is higher and sharper than the distal marginal ridge. The anterior fovea is a short, buccolingually oriented longitudinal groove restricted to the buccal half of the tooth. It is outlined by the mesial aspect of the mesial accessory crest and the mesial marginal ridge and it is continuous with the longitudinal fissure. The posterior fovea is a pit at the end of the longitudinal groove. Buccally, the tooth has very little cervical prominence. The distobuccal groove is more developed than the mesiobuccal groove though both fade

at about midcrown. There are no lingual grooves.

U.W. 110-5: RM¹ crown

This maxillary right first permanent molar consists of an unworn but completed crown with its roots broken off at the cervix (Figure 4). The completion of the crown and the fractured cervix suggest a degree of root development that would be consistent with at least gingival eruption (Cofran and Walker 2017). The crown has a rhomboidal shape with a distolingual projection of the hypocone. Four principal cusps are present. In projected area, the cusps are arranged as protocone>metacone>paracone>hypocone. Two accessory cusps are evident on the mesial marginal ridge. The cusp apices are widely spaced and positioned at the edge of the occlusal margin. On the mesial paracone crest, near the apex of the cusp, there is a rounded accessory crest that forms the distal boundary of the anterior fovea. The mesial marginal ridge is low and weakly developed. The posterior fovea is a small expansion of the fissure separating the hypocone from the metacone. The buccal groove is shallow and broad and extends from the occlusal margin to the cervix. The lingual groove is a deep narrow cleft that extends only about halfway up the face. A cervical prominence is evident on the buccal and lingual faces. The cervical line extends superiorly at the lingual groove and forms a projection of enamel between the roots on the lingual face. There is a faint Carabelli's feature which manifests as an obliquely orientated crest on the mesiolingual corner of the crown.

U.W. 110-14: RI¹ crown

This maxillary right first incisor consists of an unworn crown (Figure 5). A small portion of root remains on the mesial side of the tooth at the cervix while, due to damage, only a sliver of root remains on the distal edge. There is no incisal wear, and three faint mammelons are present on the incisal edge. The mesial crown corner is more sharply angled compared to the more gently rounded distal-incisal corner, and the distal incisal margin is more steeply angled, resulting in a crown height that is shorter distally than me-



Figure 3. A) Locality U.W. 110-2 right maxillary fourth premolar germ in buccal, lingual, distal, and mesial views. B) U.W. 110-2 (left) in occlusal view compared to RP4 from the Dinaledi Chamber, U.W. 101-334 (right).



Figure 4. A) Locality U.W. 110-5 right maxillary first molar in buccal, lingual, distal, and mesial views. B) U.W. 110-5 (left) in occlusal view compared to RM1 from the Dinaledi Chamber, U.W. 101-344 (right).



Figure 5. A) Locality U.W. 110-14 right maxillary first incisor germ in labial, distal, and mesial views. B) Lingual view of U.W. 110-14 (left) compared to R11 from the Dinaledi Chamber, U.W. 101-038 (right).

sially. The mesial and distal crown margins taper towards the cervix. The labial face is minimally curved mesiodistally and incisocervically, while the lingual face is more curved mesiodistally and incisocervically. The mesial marginal, median, and distal marginal ridges on the labial face are weakly developed. On the lingual face the mesial and distal marginal ridges are weakly defined, with the distal marginal ridge being more clearly expressed, and the median ridge fades from low near the cervical margin to flat near the incisal margin. The lingual tubercle is offset mesially, takes up a large part of the lingual face, and is continuous with the mesial marginal ridge. Despite some damage at the cervix, the cervical line appears straight. No cervical prominence is apparent on the labial face.

U.W. 110-15: RI²

This maxillary right second incisor is represented by an unworn crown with no root development (Figure 6). Two faint mammelons are present on the incisal edge. The mesial crown corner is more sharply angled compared to the more gently rounded distal-incisal corner, and the distal incisal margin is more steeply angled. The mesial and distal crown margins taper gently towards the cervix. The labial face is minimally curved mesiodistally and incisocervically, while the lingual face is more curved in both directions. Neither the cervical prominence nor mesial and distal marginal ridges are apparent on the labial face. On the lingual face the mesial and distal marginal ridges are weakly defined, with the mesial marginal ridge being more clearly

expressed, and there is no indication of a median ridge. Both ridges merge seamlessly with the lingual tubercle, the latter is offset distal to the crown midpoint and restricted to the base of the tooth near the cervix. The cervical line appears straight.

U.W. 110-17: Ldm²

This specimen is a maxillary second deciduous left molar, consisting of a crown and broken and fragile roots (Figure 7). Four principal cusps are present. The tooth has moderate wear that has blunted the cusps. Wear facets are present on all cusps, and a large pit of dentine exists on the protocone while smaller ones are visible on the paracone and hypocone. The tooth has an elliptical mesial interproximal facet but no distal interproximal facet. The crown is rhomboidal in shape with a mesiobuccal projection of the paracone and distolingual extension of the hypocone. The paracone is positioned slightly mesial to the protocone. In projected area, the cusps are arranged as protocone>paracone>metacone>hypocone. The cusp apices are widely spaced and positioned at the edge of the occlusal margin. A faint accessory crest emanates from the mesial aspect of the paracone, becoming the distal margin of the anterior fovea. The anterior fovea is a short buccolingually oriented groove. The mesial marginal ridge is thicker and higher than the distal marginal ridge, and the posterior fovea is represented by a small, circular pit at the terminus of the nearly obliterated fissure separating the hypocone from the metacone. The tooth exhibits a strong epicrista. Buccally, there is a weak cervical

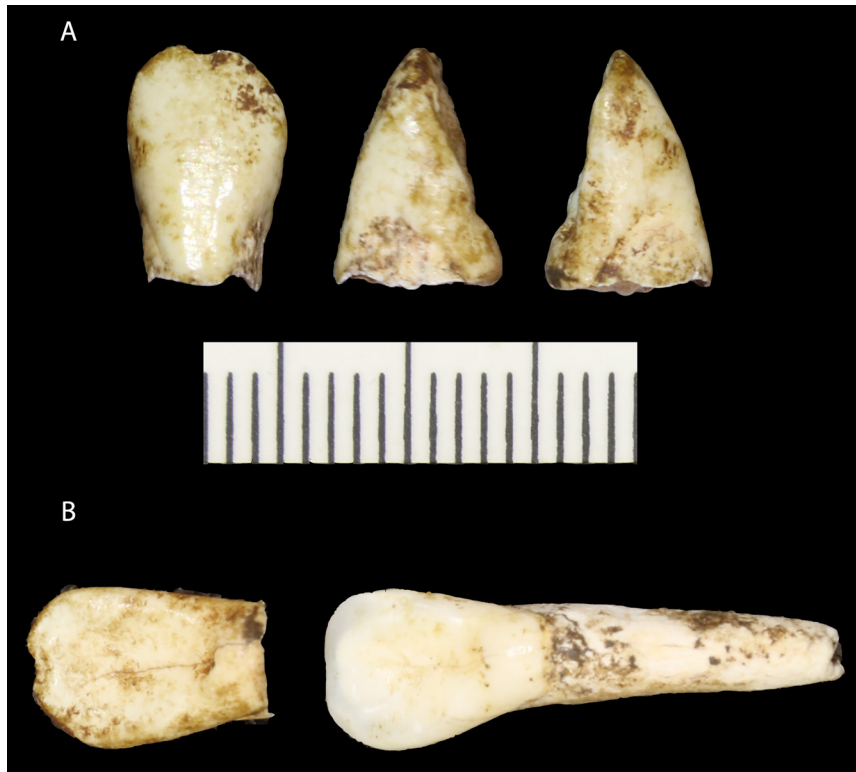


Figure 6. A) Locality U.W. 110-15 right maxillary second incisor germ in labial, distal, and mesial views. B) Lingual view of U.W. 110-15 (left) compared to RI2 from Dinaledi Chamber, U.W. 101-073 (right).



Figure 7. A) Locality U.W. 110-17 left maxillary deciduous second molar in buccal, lingual, distal, and mesial views. B) U.W. 110-17 (left) in occlusal view compared to Ldm2 from the Dinaledi Chamber, U.W. 101-1376 (right).

prominence and a small peak in the enamel between the roots. The shallow buccal groove is wide at the occlusal margin but disappears mid-crown. A weak cervical prominence is present on the lingual face. The lingual groove is a narrow cleft at the occlusal surface that becomes broader and fainter towards the cervix. A deep pit residing in an obliquely oriented, V-shaped Carabelli's feature is present on the mesiolingual corner. Enamel chipping occurs on the occlusal margin of the mesial marginal ridge and on the hypocone tip; the chips have smooth edges indicating they originated during life.

This deciduous molar retains evidence of three widely splayed roots. The mesiobuccal and distolingual roots are broken at the cervix and unstained by matrix. A small portion of the distobuccal root cavity is irregularly broken near the cervix and unstained by matrix. The tooth crown measures 8.6mm MD 9.7mm BL. The morphology and wear stage of the tooth are consistent with its proposed antimer, U.W. 110-1 (Rdm²). U.W. 110-17 is slightly smaller than the maxillary second deciduous molars from locality 101 (see Table 3).

CRANIAL FRAGMENTS

The cranial material collected from U.W. 110 includes 28 cranial fragments, none of which are complete bone elements. The largest is a fragment of frontal bone approximately 25mm in its maximum dimension. All of the fragments are compatible in thickness and appearance with hominin cranial fragments, although some are too small to allow definitive identification to element or side. Most of the specimens are relatively thin (<4mm) fragments of cranial vault, and where they can be identified they are parietal or frontal fragments, with a few exceptions noted below. The fragments are listed in Table 2.

The largest cranial fragment is part of a cluster of ten bones designated as U.W. 110-13. It is a frontal bone fragment including a portion of the right orbit, a small adjacent portion of the frontal squama, and the superiormost part of the interorbital pillar (Figure 8). The external surface of the inferiormost portion of this fragment has eroded, exposing some underlying cancellous bone. Externally, the fragment includes the superior border of the right orbit, from the medial corner of the orbit to approximately midorbit. The orbital border is relatively sharp, and no supraorbital torus development is evident. Internally, the internal frontal crest is visible with the most medial portions of both left and right anterior cranial fossae flanking it. The internal frontal crest is slightly asymmetrically positioned, and the right anterior cranial fossa is deeper and more concave than the left side, indicative of a right frontal petalia. No frontal sinus is present. The thickness of this fragment at glabella is 3.5mm. We interpret the morphology of this fragment as compatible with a young immature individual and consider evidence about its developmental age below (see Discussion).

Four additional cranial fragments surrounding bregma can be refit. Three of these fragments are also from the U.W. 110-13 bone cluster, including two small adjoining frag-

ments of the frontal that together present a small portion of the coronal suture, and one small (<10mm) fragment with both coronal and sagittal suture remnants, representing the anteromedial corner of the right parietal. An additional fragment from a cluster of bones referred to as U.W. 110-16 represents the anteromedial corner of the left parietal; this fragment conjoins both the frontal (U.W. 110-13) and right parietal (U.W. 110-116) fragments. Together, these fragments comprise an area surrounding bregma that is approximately 35mm in both anteroposterior and transverse dimensions. The thickness at bregma is 3mm. Additionally, a 20mm fragment from U.W. 110-6 is compatible with, and may conjoin with, the lateral border of the left parietal fragment, although this refit is uncertain. This fragment includes a suture along one side that may be interpreted as part of the coronal suture on the left side.

An additional morphologically informative fragment in the U.W. 110-6 bone cluster represents a portion of the left sphenoid. This specimen has an external and internal surface and includes an oval-shaped foramen, which is likely the foramen ovale. This piece does not refit any other fragment in the U.W. 110 collection and is compatible in size and preservation with the rest of the material.

Figure 9 illustrates a 3D reconstruction of the adjoining fragments together with the larger fragment from U.W. 110-13 that represents the right supraorbital and interorbital region. Elements were mirrored in 3D to approximate the missing side, with small areas of overlap at bregma and glabella permitting estimation of the curvature across the midline. This reconstruction is pictured together with the more complete adult specimens of *H. naledi*, DH3 and LES1, both of which were reconstructed using similar techniques and mirrored elements (see Figure 9). The spatial relation between the glabellar fragment and the conjoined fragments at bregma was estimated by comparison with other immature fossil specimens, including Taung (*Australopithecus africanus*), SK 54 (commonly attributed to *Paranthropus robustus*) and Mojokerto (*H. erectus*) (Figure 10). As these comparative samples represent varied developmental ages in species with different endocranial volumes, comparison with them can provide only a rough idea of the overall dimensions of the U.W. 110 frontal. However, they are sufficient to show that the preserved portions of the U.W. 110 frontal are broadly similar in curvature and dimensions to the immature specimens of *Australopithecus*, *Paranthropus*, and *H. erectus*.

TAPHONOMY AND CONTEXT

The contextual evidence of the U.W. 110 locality is enriched by the identification of this immature individual. Without further investigation, including excavation in this locality, which presents challenges, it is not known whether additional remains of this individual or others may be present. However, the results of surface collection at U.W. 110 are quite different from the commingled surface collection within the Dinaledi Chamber proper. U.W. 110's situation appears more similar to the U.W. 102b area of the Lesedi Chamber, in which cranial fragments and teeth from a sin-

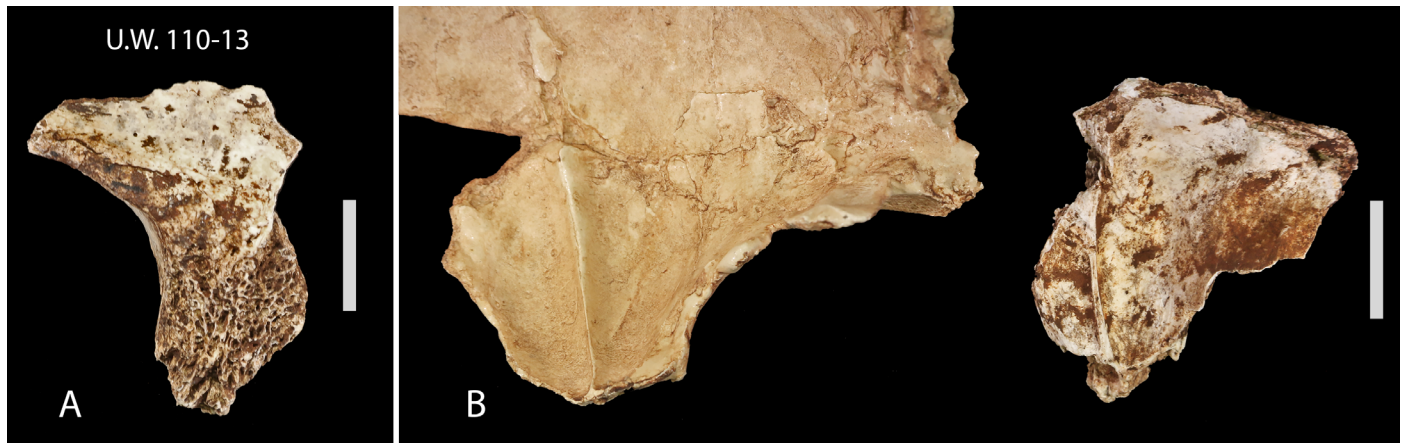


Figure 8. A) External view of U.W. 110-13 frontal specimen. B) Internal view of U.W. 110-13 (right side of panel next to another specimen demonstrating the frontal crest and anterior cranial fossae (left side of panel). The anterior cranial fossa on the right side appears slightly more anteriorly placed, possibly reflecting a right frontal petalia.

gle, immature individual were found both on the surface and in shallow, subsurface contexts in sediments that rested on a horizontal chert shelf approximately 80cm above the cave floor (Hawks et al. 2017). The U.W. 110 locality is difficult to access, in a narrow fracture passage at least 13 meters from the original 2013–2014 excavation unit in the Dinaledi Chamber.

The fossils from U.W. 110 are visually similar to those recovered from the Dinaledi and Lesedi Chambers in degree

of mineralization and in surface preservation and condition (Dirks et al. 2015; Hawks et al. 2017). This material, like that in the Dinaledi and Lesedi Chambers, has surfaces that are mildly-to-moderately weathered, mineral stained, cracked and broken (with attendant sediment infilling), and shows some evidence of modification from invertebrate activity. As with previously recovered hominin fossils from Rising Star (Dirks et al. 2015), the condition of the material can be classified as good (McKinley [2004] Grades 3 and 4), such

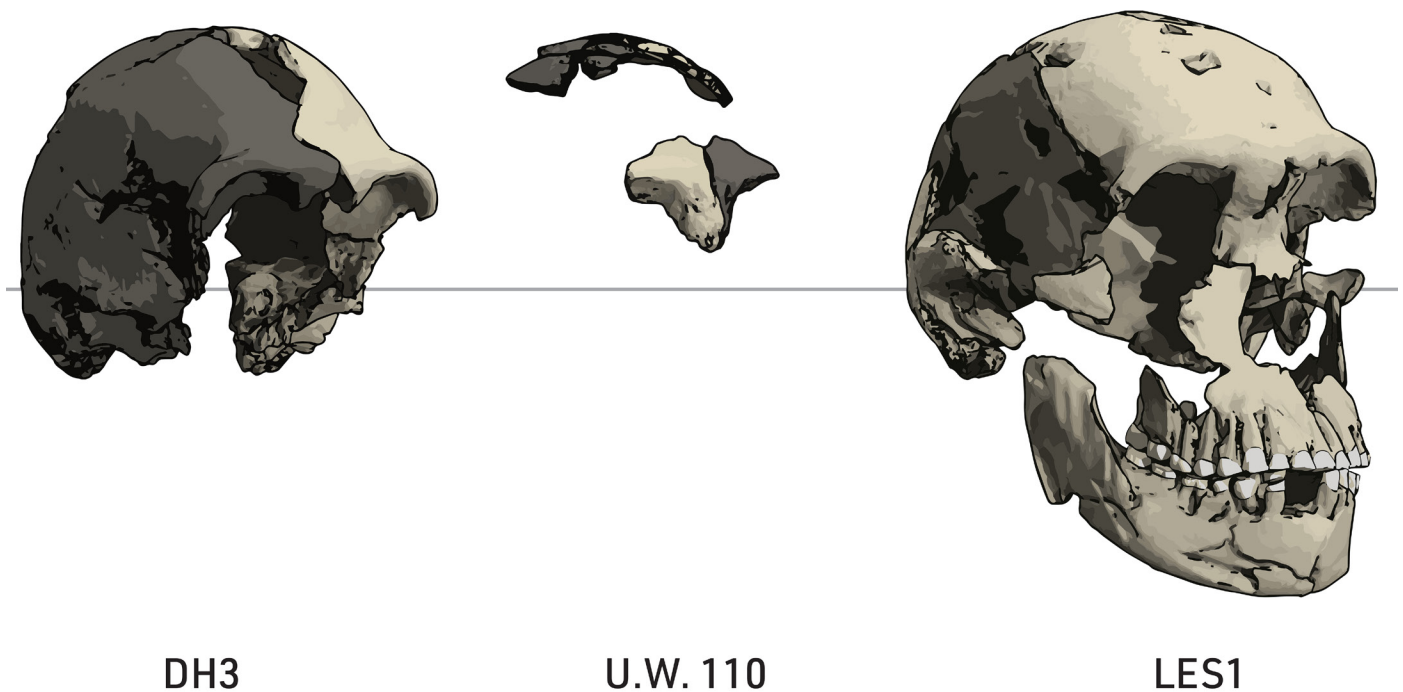


Figure 9. 3D reconstruction of the U. W. 110-13 and U.W. 110-16 conjoining fragments and the larger fragment from U.W. 110-13 that represents the left supraorbital and interorbital region. Each element was mirrored in 3D to approximate the missing right side (center). Reconstruction is pictured together with the more complete adult specimens of *H. naledi*, DH3 (left) and LES1 (right), both with similar reconstruction based upon mirrored elements.

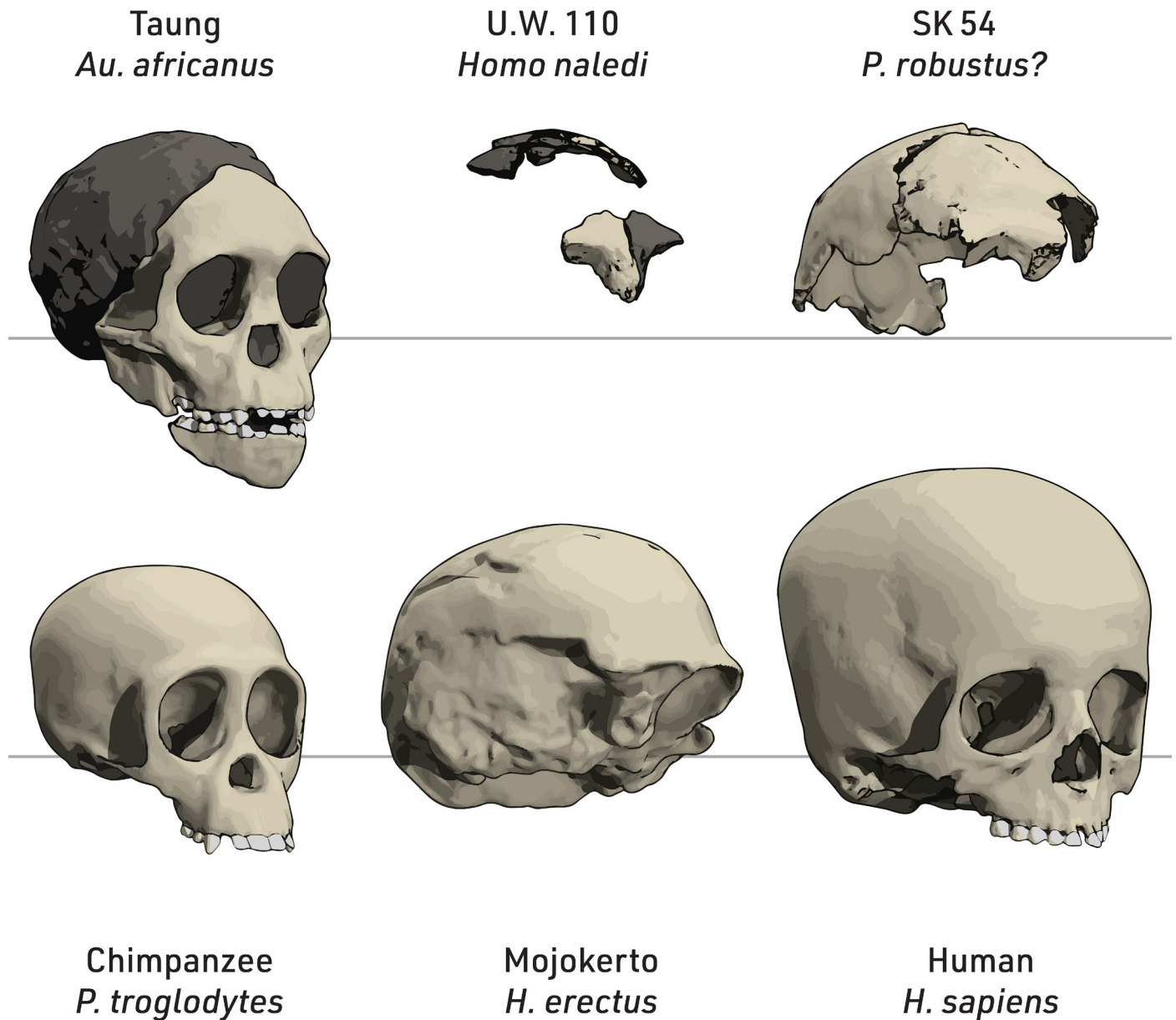


Figure 10. 3D reconstruction of the immature individual from locality U.W. 110 with Taung (*Au. africanus*), SK 54 (usually attributed to *Paranthropus robustus*), Mojokerto (*H. erectus*), chimpanzee (*P. troglodytes*), and human (*Homo sapiens*) for comparison.

that surface morphology is preserved on some specimens, but the surfaces display ubiquitous, yet varying, degrees of cortical removal, post-mortem fracturing, and striations and pitting. Evidence of invertebrate modification in the form of small pits (possibly produced by gastropod radulae) is common in the Dinaledi fossil assemblage, and can also be seen in specimens U.W. 110-3, U.W. 110-10, U.W. 110-13, and U.W. 110-16.

In addition, nine specimens from U.W. 110 (U.W. 110-3, -4, -7, -8, -10, -11, -12, -13, and -16) exhibit manganese staining similar to that described in Dirks et al. (2015). Differential weathering and mineral staining in these cases suggest breakage occurring early in the depositional his-

tory of the element, followed by differential degrees of surface exposure of the conjoining fragments (see Dirks et al. 2015). Despite broad similarities in taphonomy, the site formation processes in the Rising Star cave are complex and, at present, the temporal and depositional relationships between the hominin fossil-bearing localities (including the Dinaledi and Lesedi Chambers) remains unknown.

DISCUSSION

All of the cranial fragments and dental material from U.W. 110 are consistent with a single, immature individual. None of the elements are duplicated and all represent a similar developmental age. We therefore present the hypothesis

that this locality preserves parts of a single immature cranium. We refer to this individual as the U.W. 110 individual and consider the total evidence about its biology. The dental evidence is more definitive about developmental stage and morphological status, while the cranial evidence provides new information about the morphology of immature *H. naledi*.

The dental morphology of the U.W. 110 individual is consistent with that of other immature *H. naledi* remains from elsewhere in the Rising Star cave system. Regarding the permanent dentition, the mesiodistal and buccolingual (or labiolingual) crown dimensions of the teeth all fall within the range of the existing *H. naledi* dental sample (see Table 2). The incisors are similar to those from the Dinaledi (U.W. 101) and Lesedi (U.W. 102) samples in that they lack prominent incisocervical crown curvature, are not shoveled, and have no prominent crests on their lingual surfaces. The teeth also have broad and uninflated lingual cervical prominences. The U.W. 110-2 RP⁴ resembles those from the Dinaledi Chamber in having a paracone that is slightly larger than the protocone, a protocone apex that is mesially positioned relative to the apex of the paracone, buccal grooves that are weakly developed, and distal grooves that are deeper than the mesial grooves. The U.W. 110-5 RM¹ is similar to others of *H. naledi* in crown outline shape, cusp area, and in possessing a small, isolated Carabelli's feature that does not intersect the buccal groove.

The two deciduous maxillary molars from U.W. 110 (U.W. 110-1 and U.W. 110-17) are similar to each other in morphology, development, and lack of a distal interproximal facet. Their morphology is consistent with the teeth being antimeres. The Dinaledi Chamber dental sample includes four dm²s, all of which are consistent in having four well-developed cusps, lacking a C5, strongly expressing an epicrista, and exhibiting cusps that are widely spaced and oriented at the edge of the occlusal margin (Bailey et al. 2019). The teeth also share a moderate, V-shaped Carabelli's feature. U.W. 110-1 and U.W. 110-17 share the morphology of these *H. naledi* specimens. While many species (e.g., *H. erectus*, Zanolli et al. 2012) are represented by a comparatively small number of deciduous teeth, the growing sample from the Rising Star cave system provides some understanding of the range of variation, or lack thereof, among the second maxillary deciduous molars in this hominin species.

Enamel chipping is evident on both of the deciduous molars, U.W. 110-1 and U.W. 110-17. One other deciduous *H. naledi* tooth, U.W. 101-384 (Rdm²) from the Dinaledi Chamber, also exhibits enamel chipping. Towle et al. (2017) documented a high percentage (44%) of chipping in the permanent teeth from the Dinaledi Chamber, suggesting that this chipping was likely caused by a diet including hard foods, grit, or other inedible contaminants. This high percentage of chipping is unique within the African hominin fossil record. Regardless of the cause of the enamel chipping, the pattern is evident in both the U.W. 110 dentition and the Dinaledi Chamber dental material.

The U.W. 110 individual is at the developmental stage

corresponding with M¹ eruption. The U.W. 110-5 RM¹ has no obvious occlusal wear, but the completion of the crown and the fractured cervix suggest the roots were well developed and the tooth was in the process of erupting. The lack of distal interproximal facets on the two deciduous molars is consistent with an adjacent but newly erupted M¹. The deciduous molars of the U.W. 110 individual are moderately worn. The four permanent teeth are unworn, and none of them retain roots.

In comparison to the immature hominin remains from the Dinaledi and Lesedi Chambers, we suggest that the U.W. 110 individual fits the "early juvenile" age class (Bolter et al. 2018). A minimum of four other individuals assigned to this developmental stage are known from the Dinaledi and Lesedi Chambers. The young juvenile from the Lesedi Chamber, represented by the U.W. 102b-438 mandibular fragment, is the developmentally most similar to the U.W. 110 individual. In this specimen, the RP₄ crown is partially formed and in the crypt; although no permanent RM₁ was recovered, the alveolus retains deep root wells that are consistent with the permanent molar having erupted. Associated, but disarticulated from the U.W. 102b-438, are two incisor crowns, unworn and unerupted, LI₁ U.W. 102b-515 and RI₁ U.W. 102b-178. Both these mandibular incisors have complete but unworn crowns, comparable to the maxillary incisors U.W. 110-14 and U.W. 110-15. The U.W. 110 individual represents an older developmental stage than the U.W. 101-1400 hemi-mandible from the Dinaledi Chamber, which is associated with the most complete *H. naledi* deciduous dentition (Bolter et al. 2018; Cofran and Walker 2017). The U.W. 110 individual has substantial development of the RP⁴ crown, while there is no LP₄ crown development evident in U.W. 101-1400. The U.W. 110-5 permanent RM¹ exhibits root development and a more complete crown than the M₁ associated with U.W. 101-1400.

The 28 cranial fragments are less diagnostic than the dentition, particularly since no previous immature diagnostic cranial vault bones of *H. naledi* have been identified (Hawks et al. 2017; Laird et al. 2017). The cranial bones are compatible with the general morphology of hominin vault fragments as opposed to non-hominin fauna. On three of the cranial bones, U.W. 110-6, U.W. 110-7 and U.W. 110-16, evidence of unfused sutures is present, consistent with a young juvenile. Unlike thin, single layer cortices of infant cranial bones, U.W. 110 vault fragments exhibit thickened, double layers, indicative of the development of diplöe (Crist et al. 1997). As noted earlier, the refit vault fragments comprise the area surrounding bregma, including small pieces of frontal and both left and right parietals. Figures 9 and 10 illustrate the anatomical configuration together with the substantial U.W. 110-13 fragment that includes glabella. These portions give an impression of the overall frontal morphology of this immature individual. This model was used to compare the U.W.110 individual to other hominin specimens (see Figures 9 and 10). The evidence is insufficient to provide an accurate estimate of endocranial volume, but the radius of curvature of the endocranial sur-

face at bregma is comparable to immature hominins with endocranial volumes in the 450–650ml range, such as the Taung specimen and the endocranial volume predicted for the newly described DNH134 specimen attributed to *H. erectus* (Herries et al. 2021). This young juvenile *H. naledi*, with its right first permanent molar in gingival eruption, would be predicted to have 90–95% of its brain growth completed (McCarthy and Zimel 2020). This is compatible with the known range of adult *H. naledi* endocranial volumes at 480–610cc (Hawks et al. 2017).

In sum, the identifiable craniodental remains from U.W. 110 are consistent with *H. naledi*. No features in this sample preclude this diagnosis. Thus, we hypothesize that these remains represent the first juvenile cranial remains with diagnostic features recovered for *H. naledi*.

We hypothesize that the cranial remains and teeth that we have collected at U.W. 110 have resulted from *in situ* fragmentation of a partial or complete cranium deposited in this remote location. We regard it as likely that some hominin agency was involved in the deposition of the cranial material.

CONCLUSION

The new fossil bearing locality provides important information about a third deposit with *H. naledi* fossils within the greater Rising Star cave system. Like the other known *H. naledi* localities, U.W. 110 is difficult to access. The fossils collected from this locality represent a partial calvaria of a single immature individual of *H. naledi*. This craniodental individual contributes to our understanding of the ontogeny of *Homo naledi*, adding an additional immature specimen for a total of five young juveniles represented at localities within the Rising Star cave system.

The depositional context of U.W. 110 exhibits some differences from that of the Dinaledi Chamber material described to date and is similar in some ways to the situation in the Lesedi Chamber. The results of this research support the hypothesis that the deposition of fossil hominin material in the Rising Star cave system was a complex, multi-event process. The fossils from the new locality are similar in preservation to other previously recovered *H. naledi* fossils. The new fossils further support a single hominin species representation in the Rising Star cave system, with consistent morphology for *H. naledi* across the multiple localities from which fossils have now been recovered.

ACKNOWLEDGEMENTS

The authors thank the editor and reviewers who provided valuable feedback and comments on the manuscript. Funding for this research was provided by the National Geographic Society, the Lyda Hill Foundation, the South African National Research Foundation, the South African Centre for Excellence in Palaeosciences, The University of the Witwatersrand, the Vilas Trust, the Fulbright Scholar Program, Louisiana State University, North Carolina State University, the Texas A&M University College of Liberal Arts Seed Grant program and the Texas A&M College of Liberal Arts Cornerstone Faculty Fellowship. We wish to

thank the Jacobs Family and later the Lee R. Berger Foundation for Exploration, for access to the site, and the South African Heritage Resource Agency and Cradle of Humankind UNESCO World Heritage Site Management Authority for issuing the various permits required for this work, including the excavation permit (PermitID: 952). We would also like to thank the University of the Witwatersrand and the Evolutionary Studies Institute, as well as the South African National Centre of Excellence in Palaeosciences, for curating the material and for hosting the authors while they were studying the material, with thanks to Dr. Bernhard Zipfel for facilitating the research. Finally, we thank Katrina Schroeffer.

REFERENCES

- Bailey, S.E., Brophy, J.K., Moggi-Cecchi, J., and Delezene, L.K. 2019. The deciduous dentition of *Homo naledi*: A comparative study. *Journal of Human Evolution* 136, 102655.
- Berger, L.R., Hawks, J., de Ruiter, D.J., Churchill, S.E., Schmid, P., Delezene, L.K., Kivell, T.L., Garvin, H.M., Williams, S.A., DeSilva, J.M., Skinner, M.M., Musiba, C.M., Cameron, N., Holliday, T.W., Harcourt-Smith, W., Ackermann, R.R., Bastir, M., Bogin, B., Bolter, D., Brophy, J., Cofran, Z.D., Congdon, K.A., Deane, A.S., Dembo, M., Drapeau, M., Elliott, M.C., Feuerriegel, E.M., Garcia-Martinez, D., Green, D.J., Gurtov, A., Irish, J.D., Kruger, A., Laird, M.F., Marchi, D., Meyer, M.R., Nalla, S., Negash, E.W., Orr, C.M., Radović, D., Schroeder, L., Scott, J.E., Throckmorton, Z., Tocheri, M.W., VanSickle, C., Walker, C.S., Wei, P., and Zipfel, B. 2015. *Homo naledi*, a new species of the genus *Homo* from the Dinaledi Chamber, South Africa. *eLife* 4, e09560.
- Bolter, D.R., Hawks, J., Bogin, B., and Cameron, N. 2018. Palaeodemographics of individuals in Dinaledi Chamber using dental remains. *South African Journal of Science* 114, 37–42.
- Bolter, D.R. and Cameron, N. 2020. Utilizing auxology to understand ontogeny of extinct hominins: A case study on *Homo naledi*. *American Journal of Physical Anthropology* 173, 368–380.
- Bolter, D.R., Elliott, M., Hawks, J., and Berger, L. 2020. Immature remains and the first partial skeleton of a juvenile *Homo naledi*, a late Middle Pleistocene hominin from South Africa. *PLoS One* 15(4), e0230440.
- Cofran, Z. and Walker, C.S. 2017. Dental development in *Homo naledi*. *Biology Letters* 13(8), 20170339.
- Crist, T.A., Washburn, A., Park, H., Hood, I., and Hickey, M.A. 1997. Cranial bone displacement as a taphonomic process in potential child abuse cases. In Haglund, W., Sorg, M. (eds.), *Forensic Taphonomy: the postmortem fate of human remains*. CRC Press, Florida, pp. 319–336.
- de Ruiter, D.J., Laird, M.F., Elliott, M., Schmid, P., Brophy, J., Hawks, J., and Berger, L.R. 2019. *Homo naledi* cranial remains from the Lesedi chamber of the rising star cave system, South Africa. *Journal of Human Evolution* 132, 1–14.
- Dirks, P.H.G.M., Berger, L.R., Roberts, E.M., Kramers, J.D.,

- Hawks, J., Randolph-Quinney, P.S., Elliott, M., Musiba, C.M., Churchill, S.E., de Ruiter, D.J., Schmid, P., Backwell, L.R., Belyanin, G.A., Boshoff, P., Hunter, K.L., Feuerriegel, E.M., Gurtov, A., Harrison, J.d.G., Hunter, R., Kruger, A., Morris, H., Makhubela, T.V., Peixotto, B., and Tucker, S. 2015. Geological and taphonomic context for the new hominin species *Homo naledi* from the Dinaledi Chamber, South Africa. *eLife* 4, e09561.
- Dirks, P.H.G.M., Roberts, E.M., Hilbert-Wolf, H., Kramers, J.D., Hawks, J., Dosseto, A., Duval, M., Elliott, M., Evans, M., Grün, R., Hellstrom, J., Herries, A.I.R., Joannes-Boyau, R., Makhubela, T.V., Placzek, C.J., Robbins, J., Spandler, C., Wiersma, J., Woodhead, J., and Berger, L.R. 2017. The age of *Homo naledi* and associated sediments in the Rising Star Cave, South Africa. *eLife* 6, e24231.
- Elliott, M.C., Makhubela, T.V., Brophy, J.K., Churchill, S.E., Peixotto, B., Feuerriegel, E.M., Morris, H., Van Rooyen, D., Ramalepa, M., Tsikoane, M., Kruger, A., Spandler, C., Kramers, J., Roberts, E., Dirks, P.H.G.M., Hawks, J., and Berger, L.R. 2021. New explorations and excavations in the Dinaledi Subsystem, Rising Star Cave. *PaleoAnthropology* 2021:1, 15–22.
- Feuerriegel, E.M., Green, D.J., Walker, C.S., Schmid, P., Hawks, J., Berger, L.R., and Churchill, S.E. 2017. The upper limb of *Homo naledi*. *Journal of Human Evolution* 104, 155–173.
- Feuerriegel, E.M., Voisin, J.-L., Churchill, S.E., Haeusler, M., Mathews, S., Schmid, P., Hawks, J., and Berger, L.R. 2019. Upper limb fossils of *Homo naledi* from the Lesedi Chamber, Rising Star System, South Africa. *PaleoAnthropology* 2019, 311–349.
- Hawks, J., Elliott, M., Schmid, P., Churchill, S.E., de Ruiter, D.J., Roberts, E.M., Hilbert-Wolf, H., Garvin, H.M., Williams, S.A., Delezene, L.K., Feuerriegel, E.M., Randolph-Quinney, P., Kivell, T.L., Laird, M.F., Tawane, G., DeSilva, J.M., Bailey, S.E., Brophy, J.K., Meyer, M.R., Skinner, M.M., Tocheri, M.W., VanSickle, C., Walker, C.S., Campbell, T.L., Kuhn, B., Kruger, A., Tucker, S., Gurtov, A., Hlophe, N., Hunter, R., Morris, H., Peixotto, B., Ramalepa, M., Rooyen, D.V., Tsikoane, M., Boshoff, P., Dirks, P.H.G.M., and Berger, L.R. 2017. New fossil remains of *Homo naledi* from the Lesedi Chamber, South Africa. *eLife* 6, e24232.
- Herries, A.I., Martin, J.M., Leece, A.B., Adams, J.W., Boschian, G., Joannes-Boyau, R., Edwards, T.R., Mallett, T., Massey, J., Murszewski, A., and Neubauer, S. 2020. Contemporaneity of *Australopithecus*, *Paranthropus*, and early *Homo erectus* in South Africa. *Science* 368, eaaw7293.
- Kivell, T.L., Deane, A.S., Tocheri, M.W., Orr, C.M., Schmid, P., Hawks, J., Berger, L.R., and Churchill, S.E. 2015. The hand of *Homo naledi*. *Nature Communications* 6, 8434.
- Laird, M.F., Schroeder, L., Garvin, H.M., Scott, J.E., Dembo, M., Radovčić, D., Musiba, C.M., Ackermann, R.R., Schmid, P., Hawks, J., and Berger, L.R. 2017. The skull of *Homo naledi*. *Journal of Human Evolution* 104, 100–123.
- McCarthy, R.C. and Zimel, E. 2020. Revised estimates of Taung's brain size growth. *South African Journal of Science* 116, 1–7.
- McHenry, H.M., Corruccini, R.S., Howell, F.C. 1976. Analysis of an early hominid ulna from the Omo basin, Ethiopia. *American Journal of Physical Anthropology* 44, 295–304.
- McKinley, J.I. 2004. Compiling a skeletal inventory: disarticulated and co-mingled remains. In Brickley M., McKinley, J.I. (eds.), *Guidelines to the Standards for Recording Human Remains*. Institute of Field Archaeologists Technical Paper No. 7, 14–17.
- Randolph-Quinney, P.S. 2015. A new star rising: Biology and mortuary behavior of *Homo naledi*. *South African Journal of Science* 111, 1–4.
- Schroeder, L., Scott, J.E., Garvin, H.M., Laird, M.F., Dembo, M., Radovčić, D., Berger, L.R., de Ruiter, D.J., and Ackermann, R.R. 2017. Skull diversity in the *Homo* lineage and the relative position of *Homo naledi*. *Journal of Human Evolution* 104, 124–135.
- Towle, I., Irish, J.D., and De Groote, I. 2017. Behavioral inferences from the high levels of dental chipping in *Homo naledi*. *American Journal of Physical Anthropology* 164(1), 184–192.
- White, T.D. 1992. *Prehistoric Cannibalism at Mancos 5MT-UMR-2346*, Princeton University Press, Princeton, New Jersey.
- Zanolli, C., Bondioli, L., Mancini, L., Mazurier, A., Widianto, H., and Macchiarelli, R. 2012. Brief communication: two human fossil deciduous molars from the Sangiran Dome (Java, Indonesia): outer and inner morphology. *American Journal of Physical Anthropology* 147(3), 472–481.